Microalgae Cultivation (*Chlorella vulgaris*) within Nanocellulose-based Biomaterial Ink for 3D Bioprinting

Wan Nazihah Liyana Wan Jusoh [a,b,*] Grace Toh Jia Ern,[a,b] Nazlina Haiza Mohd Yasin,[c] Peer Mohamed Abdul,[a,b] Mohd Sobri Takriff [a,b,d] and Mohd Shaiful Sajab [a,b,*]

** Corresponding authors: nazihahliyana.j@gmail.com; mohdshaiful@ukm.edu.my*

DOI: 10.15376/biores.21.4.9761-9779

GRAPHICAL ABSTRACT

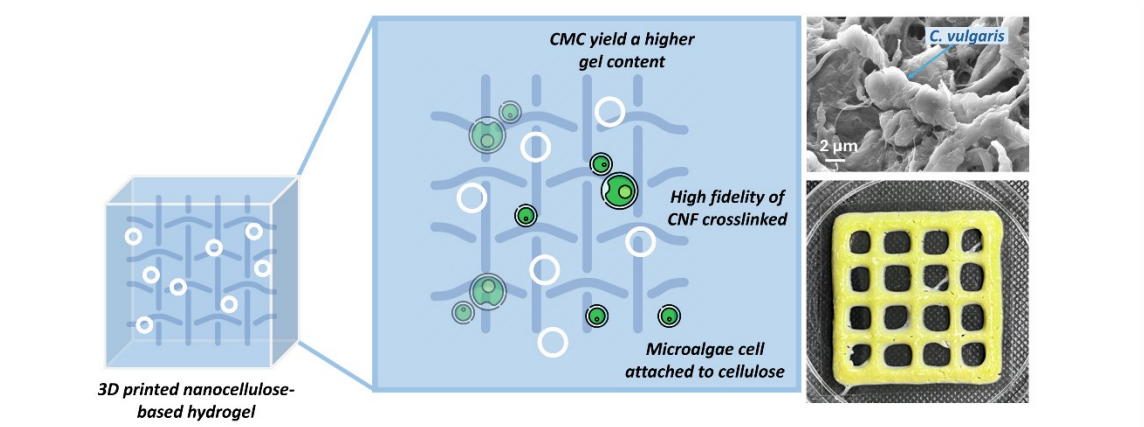

Microalgae cultivation (*Chlorella vulgaris*) within nanocellulose-based biomaterial ink

Microalgae Cultivation (*Chlorella vulgaris*) within Nanocellulose-based Biomaterial Ink for 3D Bioprinting

Wan Nazihah Liyana Wan Jusoh [a,b,*] Grace Toh Jia Ern,[a,b] Nazlina Haiza Mohd Yasin,[c] Peer Mohamed Abdul,[a,b] Mohd Sobri Takriff [a,b,d] and Mohd Shaiful Sajab [a,b,*]

Advances in microtechnology have progressively improved cultivation methods, providing significant benefit through hydrogel immobilization, which enables more controlled nutrient delivery and a conducive environment. In this work, *Chlorella vulgaris*, a microalgal species, was used to investigate the cell cultivation and optimal growth conditions within cellulose-based bioinks composed of cellulose nanofibrils (CNF) and carboxymethyl cellulose (CMC). *C. vulgaris* immobilization serves as a bioprinted living cell model focused on a plant-based system, enhancing the understanding of a modern and simplified cultivation techniques. The growth rates of *C. vulgaris* cells in CNF/CMC hydrogels were evaluated using colorimetric analysis with different cell cultivation techniques. The morphological structure was analyzed within the CNF/CMC hydrogel, *C. vulgaris* culture, and the immobilized *C. vulgaris* in the hydrogel. The optimal conditions at room temperature for *C. vulgaris* growth were established by preparing the hydrogels with varying CNF and CMC concentration ratios for subsequent 3D bioprinting processes. Remarkably, the 3D-bioprinted hydrogel with a concentration ratio of 5 wt% CNF and 5 wt% CMC demonstrated superior structural integrity, with capability for 3D printing and exceptional *C. vulgaris* cell growth rates. A green and comprehensive method of nanocellulose-based bioinks showed great properties for the application of other cells' culture with 3D bioprinting.

DOI: 10.15376/biores.21.4.9761-9779

Keywords: Additive manufacturing; Bioprinting; Cellulose; Microalgae; Compatibility

Contact information: a: Research Center for Sustainable Process Technology (CESPRO), Faculty of Engineering and Built Environment, Universiti Kebangsaan Malaysia, 43600 Bangi, Selangor, Malaysia; b: Department of Chemical and Process Engineering, Faculty of Engineering and Built Environment, Universiti Kebangsaan Malaysia, 43600 Bangi, Selangor, Malaysia; c: Department of Biological Sciences and Biotechnology, Faculty of Science and Technology, Universiti Kebangsaan Malaysia, 43600, UKM, Bangi, Selangor, Malaysia; d: Department of Mechanical and Nuclear Engineering, College of Engineering, University of Sharjah, United Arab Emirates;
** Corresponding authors: nazihahliyana.j@gmail.com; mohdshaiful@ukm.edu.my*

INTRODUCTION

Three-dimensional (3D) bioprinting shares a similar concept with 3D printing, capable of producing a scaffold in a 3D shape, but it incorporates living cells during the process to produce viable tissue and living scaffolds using bioink (Vurat *et al.* 2022). Its present applications, extending various fields, are predominantly utilized in the field of tissue engineering and regenerative medicine (Ramadan *et al.* 2021). However, it extends beyond this through the involvement of other living cells in food technology, agriculture and aquaculture biotechnology, wastewater treatment, bioenergy, and carbon management.

Bioink, a crucial component of 3D bioprinting, comprises a biomaterial that encapsulates living cells in a gel-like form. The bioink employed should offer high resolution during the 3D bioprinting process, exhibit high biocompatibility with the living cells, and maintain mechanical stability to preserve the structure of the scaffold post 3D bioprinting (Gopinathan and Noh 2018).

Bioink can be synthesized using biopolymers, with cellulose being a popular choice due to its affordability, renewability, and widespread availability as a polysaccharide (Kargarzadeh *et al.* 2017; Shaghaleh *et al.* 2018). Furthermore, cellulose possesses a robust mechanical structure and biocompatibility, particularly at the nanoscale, because of its unique properties of high surface area and strength, non-toxic and applicable for the modification according to its application (Jorfi and Foster 2015). These characteristics enable cellulose to be utilized in diverse sectors, including pharmaceuticals, tissue engineering, and halal agricultural medium (Zainal *et al.* 2019). However, when used as a pure nanocellulosic material for bioink in hydrogel fabrication, cellulose nanofibrils (CNF) have certain limitations, such as high shear-thinning property, low mechanical strength of the hydrogel, and structural shrinkage upon drying (Badhe and Nipate 2020). These limitations needs to be addressed in order to take advantage of its ability to provide an extracellular matrix (ECM)-like environment and excellent biocompatibility. As suggested by Nan *et al.* (2019), these issues can be mitigated by using a composite of CNF and carboxymethyl cellulose (CMC) to enhance the mechanical strength of the hydrogel bioink. This is attributed to the high number of carboxyl functional groups (COO-) in CMC, which can yield a higher gel content when crosslinked with calcium chloride ($CaCl_2$).

The current research and development in the field of 3D bioprinting technology faces certain challenges such as poor bioink mechanical stability, cells survival and stability, cost, and scalability. The assurance of the viability of cells within the bioprinted hydrogel for applications in biomedical, biotechnology, or environmental remediation is still pending. Therefore, the initial research utilized model microorganisms, including microalgae, the plant cell, to study cell viability and optimal growth conditions in the cellulose-based bioink. *Chlorella vulgaris*, a green microalga from the Chlorophyta division, is an ideal candidate for this research due to its fast growth rate and adaptability to changing physico-chemical conditions (Wirth *et al.* 2020). Typically, microalgae cultivation falls into two categories: open culture systems and closed culture systems. Open culture systems refer to open raceway ponds (ORW), while closed culture systems involve the use of photobioreactors (PBR) (Show *et al.* 2020). Unlike traditional techniques that culture microalgae in suspensions, this method cultures microalgae in hydrogel. Through a process called immobilization, living cells are encapsulated within a polymeric matrix that allows a nutrient-rich suspension to circulate through it (Cohen 2001).

There are various 3D bioprinting methods, including extrusion-based bioprinting (EBB), droplet-based bioprinting (DBB), and laser-assisted bioprinting (LAB). The EBB method extrudes a viscous bioink to form a continuous filament layer-by-layer through a nozzle, using pneumatic, piston, or screw forces (Landers *et al.* 2002). The liquid deposition modelling (LDM) technique employed in this study uses a motor to generate pressure during the extrusion of the liquid bioink solution. In the process of preparing hydrogel bioink, microalgae cells were directly cultivated in the hydrogel, which is a departure from traditional cultivation methods. The growth of microalgae within the hydrogel matrix is confirmed based on the green hue formation through the cultivation process, closely related to the chlorophyll, which is a green pigment. This green pigment allows for the application of the colorimetric method using RGB colour to measure cell

growth, together with a wider spectrum to capture colour variations within the cultivation period.

In this study, *C. vulgaris* was cultured in the biobased hydrogel made up of CNF and CMC. The hydrogel composition, with the presence of crosslinker and cultivation conditions, was manipulated to study the growth rates of microalgae cells, *C. vulgaris*. The optimum growth condition of *C. vulgaris* in the CNF/CMC hydrogel will be used in analysing the potential of the cells in 3D bioprinting by varying the hydrogel composition ratio. The 3D-printed microalgae scaffold with good shape fidelity is expected from the LDM printing technique.

EXPERIMENTAL

Materials

Oil palm empty fruit bunch fiber (OPEFB), was mechanically processed and passed through a mesh screen, ranging in size from 106 to 500 µm. It served as the primary raw material for the cellulose isolation and processing. The preparation of cellulose and cellulose ink required the use of 90% formic acid, 30% hydrogen peroxide (H_2O_2), iron (II) derived from iron (II) sulfate heptahydrate ($Fe_2SO_4 \cdot 7H_2O$), calcium chloride ($CaCl_2$), and sodium carboxymethyl cellulose (NaCMC), all sourced from Merck, Darmstadt, Germany. Bold's Basal Medium (BBM) is a composite of macronutrient, alkaline ethylenediaminetetraacetic acid (EDTA) solution, acidic iron solution, boron solution, and trace metal solution utilized following the previous study (Anderson 2005).

Preparation of CNF/CMC Hydrogel

Cellulose was isolated from OPEFB through a procedure that has been documented in previous research (Sajab *et al.* 2019; Mohan *et al.* 2021; Wan Jusoh *et al.* 2025). Briefly, the solution of 90% formic acid and OPEFB at ratio 30:1 was stirred at 90 °C for 2 h (IKA RCT Basic, IKA Staufen, Germany), effectively removing lignin from the biomass. The resulting supernatant and pulp were separated using vacuum filtration and washed with distilled water (IKA MVP10 Basic, IKA, Staufen, Germany). The extracted pulp underwent catalytic oxidation in hydrogen peroxide (1 to 6% w/v) and Fenton reagent and Fe(0) nanoparticles derived from iron (II) sulphate heptahydrate solution (2 to 14 mg/L) at 90 °C for 24 h to purify the fibers. A total of 1 M hydrochloric acid (HCl) was added in ~0.1 mL increments to make the solution a stable and low potential of sedimentation. The fibers were then filtered and washed until a neutral pH was achieved and chilled at ~ 4 ℃ for future use. To produce cellulose nanofibrils (CNF), the isolated cellulose fibers (0.7 wt%) were fibrillated in deionized water using a high-speed homogenizer (IKA T25 Digital, Staufen, IKA Germany) in a constant room temperature 25 °C and at 25,000 rpm rotation speed. The homogenizing process was conducted for 30 minutes in control cycle of 10 minutes to prevent hydrolysis by ensuring the temperature below 70 °C. The fibrillated cellulose was then stored at ~ 4 ℃ for further use.

Hydrogel Cultivation Parameters

C. vulgaris from *Chlorella* group was used as the microalgae species for the whole study. The BBM was utilized as the nutrient source for *C. vulgaris* cell cultivation, and is formulated in distilled water (Anderson 2005). The materials and tools used in this step were sterilized using an autoclave at 121 ℃. A 10 wt% of the *C. vulgaris* stock culture was

introduced to the sterilized BBM, and the cells in this inoculum were permitted to grow under light and aeration. The growth curve of *C. vulgaris* was determined daily using a UV spectrophotometer at wavelength of 750 nm and the color differences were observed (Yatirajula *et al.* 2019).

In the preparation of CNF/CMC hydrogel for microalgae cultivation, BBM was utilized as the solution replacing the distilled water. A 4.5 wt% CNF was incorporated and blended with the BBM solution at room temperature with the stirring rate of 1,200 rpm for a duration of 10 min. Concurrently, a 5 wt% CMC solution was formulated by dissolving NaCMC powder in the BBM solution at 60 °C, maintaining a constant stirring speed of 1,200 rpm for a duration of 30 min. The CNF/CMC hydrogel was then prepared by introducing the dissolved CMC into the CNF suspension and stirred for an additional 30 min using an overhead stirrer at 2,500 rpm for another 30 minutes.

Nanocellulose-based hydrogels were then prepared in accordance with their components and categories, as outlined in Table 1. *C. vulgaris* cells were then introduced into the hydrogel bioink at a concentration of 1.00×10^7 cells/mL for both with and without 3D bioprinting. The prepared nanocellulose-based hydrogels were molded into a square shape ($20 \times 20 \times 10$ mm^3), and the necessary crosslinking process for each category was achieved by immersing the hydrogels into a 5 wt% $CaCl_2$ solution for 10 min (Krujatz *et al.* 2015). The hydrogel was left to cultivate for a period of 10 days based on their listed conditions in Table 1. A colorimetric analysis was employed to determine the growth rate of *C. vulgaris* using red, green, and blue intensity (RGB) values. RGB is a color model, often displayed on digital screens by forming different colors through an array of red, green, and blue colors. For this study, colorimetric analysis was used to detect the color in the hydrogel and form RGB values representing the detected colors. Throughout this period, daily analyses were conducted on the physical appearance, color changes, and RGB values.

Table 1. Hydrogel Composition of Each Category

Category	Composition	Crosslinking with $CaCl_2$	Cultivation Condition
I	CNF suspension, CMC solution, *C. vulgaris* cells, BBM	No	Hydrogel left at room temperature (25 °C)
II	CNF suspension, CMC solution, *C. vulgaris* cells, BBM	Yes	Hydrogel left at room temperature (25 °C)
III	CNF suspension, CMC solution, *C. vulgaris* cells, BBM	Yes	Hydrogel immersed in BBM
IV	CNF suspension, CMC solution, *C. vulgaris* cells, BBM	Yes	Hydrogel immersed in distilled water
V	CNF suspension, CMC solution, *C. vulgaris* cells	Yes	Hydrogel immersed in BBM

3D Bioprinting Parameters

The LDM method, which uses a paste extruder, was chosen for 3D bioprinting because it works well with the liquid ink extrusion of the CNF/CMC hydrogel (Mohan *et al.* 2020). The Discov3ry paste extruder (Structur3d Printing, Kitchener, Canada) was integrated with an Ultimaker 2+ 3D printer (Ultimaker, Netherlands). Prior to 3D bioprinting, the desired three-dimensional shape was designed using computer-aided design software. The design file was saved in .stl format and converted to G-Code format using Ultimaker Cura 4.5 software (Geldermalsen, Netherlands) in accordance with the

Discov3ry configuration. To facilitate a seamless 3D bioprinting process, parameters, such as nozzle movement direction, bioink flow rate, and printing speed, were adjusted during the format conversion. A nozzle of 0.84 mm diameter was employed for all printings across different CNF/CMC concentrations, with the printing speed of 20 mm/s and flow rate of 1 mL/min.

Leveraging the optimal cultivation technique identified in the previous step, five hydrogel samples with varying CNF and CMC concentration ratios were prepared as per Table 2. A square grid shape was chosen as the design structure for 3D bioprinting analysis. The hydrogel was allowed to grow at room temperature under the presence of air and light. Daily records were maintained for 7 days using colorimetric analysis to monitor changes in the physical appearance of the bioprinting and the growth of the microalgae.

Table 2. Hydrogel Composition and Cultivation Conditions for Category I

Sample	Concentration Ratio of CNF (wt%)	Concentration Ratio of CMC (wt%)
CNF/CMC 4:5	4	5
CNF/CMC 5:5	5	5
CNF/CMC 6:5	6	5
CNF/CMC 4:6	4	6
CNF/CMC 5:6	5	6

Characterization

The rheological test was conducted using Physica MCR301 (Anton Paar, Austria) to study the shear stress and viscosity of the ink at varying shear rate. Shear rate was specified as between 0.01 and 100 s^{-1} at 25 °C, and the shear stress and viscosity were recorded. The culture media's optical density was measured using a DR1900 spectrophotometer from HACH, Colorado, USA, at a wavelength of 750 nm. To quantify the cell concentration within the hydrogel system, a colorimetric analysis was executed by monitoring color variations to quantify the concentration of a sample. A digital camera was used to detect changes in RGB values, which were then converted into concentrations using a linear equation derived from a calibration curve. The camera lens was kept at a distance of 22 cm from the sample, and all images were captured in a light box with controlled brightness. The Colorimetric Titration application (Colorimetric Titration 2021) was used to obtain the RGB value of each sample based on their respective cell concentration and color.

To gain deeper understanding of the *C. vulgaris* immobilization and growth in CNF/CMC hydrogel, a morphology test was conducted to see the attachment of cells. The structure of microalgae and CNF/CMC hydrogel was examined using an optical microscope (B-380 series, OPTIKA microscope, Bergamo, Italy). The morphology of three samples, CNF/CMC hydrogel, *C. vulgaris* culture, and immobilized *C. vulgaris* in CNF/CMC hydrogel, were analyzed using Field Emission Scanning Electron Microscopy (FESEM) (Merlin Compact, Zeiss Pvt Ltd., Oberkochen, Germany). Sample preparation was required before the analysis in which the *C. vulgaris* cells underwent critical point drying, whereas the hydrogel was freeze dried and then the samples were sputter-coated with gold before being viewed under the microscope.

ImageJ (Ver. 2.15.1) embedded in Fiji software (https://imagej.net/software/fiji/) was used as a scientific imaging analysis to analyze the real image using color analysis. This analysis simply requires the image and software for the quantification to be done

automatically (Dishon *et al.* 2022). The color channel needs to be chosen during the analysis and in this study, the green channel was the best choice due to the green color of microalgae cells. The results are presented as a black and white image, where the white color refers to the microalgae cells and black represents the biomaterial substrate.

RESULTS AND DISCUSSION

Optical Properties of *C. vulgaris* in CNF/CMC System

In the initial phase of the study, the growth of *C. vulgaris* in CNF, CMC, and CNF/CMF solutions was examined to gain insights on the cell development potential. Observations were made from the alterations in the green colour's intensity, which directly gave an indication of the cell's pigment within 5 days of cultivation (refer to Fig. 1(a)). Remarkably, *C. vulgaris* demonstrated the ability to grow and thrive in all biomaterial solutions, which was confirmed by the color shift from yellowish to green during the growth period. This suggests that the biomaterial solution exhibited low toxicity, was safe, and fostered an environment conducive to microalgae cell growth. Based on Fig. 1(a), cell growth in CNF and CNF/CMC solutions tended to occur more on the surface of the solution compared to the bottom part. However, CMC biomaterial showed uniform growth throughout the solution. The white color of CNF, in contrast to the colorless and transparent nature of CMC, also affected the transmission of light, causing microalgae in CNF to move towards the surface. Nevertheless, all biomaterial formulations supported cell growth due to their low toxicity, safety, and ability to provide a conducive environment for cells.

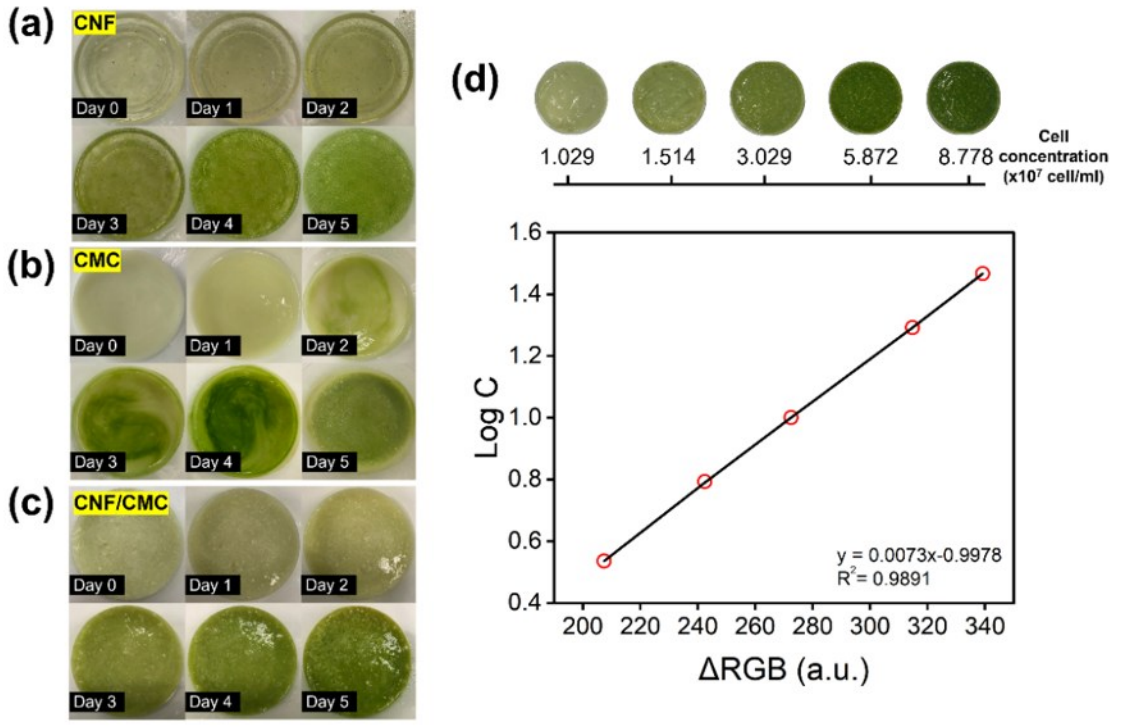

Fig. 1. Optical observation on (a-c) *C. vulgaris* within CNF, CMC, and CNF/CMC suspension for 5 days cultivation and (d) colorimetric calibration curve of CNF/CMC hydrogel at cell concentration of 1 x 10^7 cell/mL to 8.7 x 10^7 cell/mL

To further enhance the analysis, the colorimetric method, which utilizes RGB intensity values, was found to be an effective technique for examining these color changes. The RGB data can represent these three colors with numbers ranging from 0 to 225 (Hlaing *et al.* 2020; Pazzi *et al.* 2022). This technique is particularly effective for analyzing concentrations in hydrogel, as using a spectrophotometer for optical density can be challenging. Five CNF/CMC hydrogel samples, each with different cell concentrations, were prepared for analysis. A standard calibration curve of CNF/CMC hydrogel at cell concentration of 1 x 10^7 cell/mL to 9 x 10^7 cell/mL cell concentration was tabulated within log C *vs.* ΔRGB values of each sample at different concentrations (see Fig. 1(d)). This standard curve was used to analyze subsequent data and determine cell concentration values at their individual ΔRGB value obtained through colorimetric analysis. The R^2 value of 0.9891 was successfully recorded for the standard curve produced. Meanwhile, the detection limit was determined through the standard curve, which signifies the quantification limit for the CNF/CMC hydrogel during the cultivation of microalgae.

Effects of Cultivation Technique in Hydrogel System

The influence of the cultivation methodology within the hydrogel system was manifested in the physical changes of *C. vulgaris* growth in the hydrogel, as shown in Fig. 2. The physical changes observed over a span of 10 days can be attributed into two components: the structural integrity of the hydrogel and the cellular proliferation. Category I and II were fabricated in a similar condition except for the presence of the crosslinker. Structurally, on the first day, hydrogel in Category II possessed higher structural stability compared to Category I. This situation aligned with the usage and functionality of the crosslinker to improve the mechanical strength and stabilize the structure (Nasution *et al.* 2022). On the third day, the hydrogels of Categories I and II started to desiccate, potentially due to water evaporation. Conversely, the hydrogels of Categories III and IV began to disintegrate in their respective solutions on the fourth day.

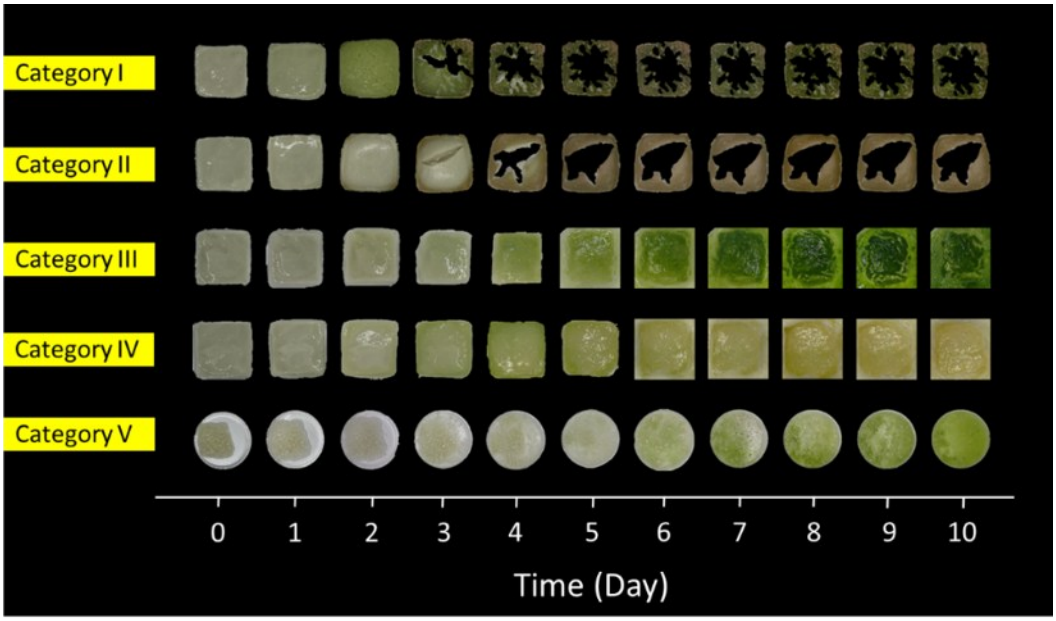

Fig. 2. Changes in the physical appearance of *C. vulgaris* growth in hydrogel at different composition and cultivation conditions

The CNF utilized did not undergo a chemical dissolution and crosslinking process, resulting in a less cohesive inner structure of the nanocellulose (Sood *et al.* 2011; Ergun *et al.* 2016; Stanbury *et al.* 2017). This less cohesive structure makes the hydrogel more prone to dissolution in the solutions. The hydrogel did not undergo a chemical dissolution and crosslinking process, as it often involves chemicals harmful to microalgae. The structure of the Category V hydrogel was not rigid from day 0, appearing to collapse and dissolve in the BBM solution. This could be attributed to non-uniform mixing during the preparation of the CMC solution, leading to a less viscous hydrogel that dissolves readily.

The proliferation of *C. vulgaris* cells can be deduced from the color shifts in the hydrogel, where an escalating green hue signifies cell growth due to chlorophyll pigments, while a transition to a whitish or yellowish hue indicates cell disruption and mortality. Hydrogels of Categories I, III, and V exhibited a progressive shift from an initial whitish hue to a greener one, indicating that the growth of *C. vulgaris* was enhanced with the addition of BBM during hydrogel preparation and cultivation. Notably, the hydrogels of Categories I and III displayed a more pronounced increase in green intensity, suggesting superior *C. vulgaris* growth in these categories.

The hydrogel of Category II did not demonstrate any discernible color change throughout the experiment, implying a lack of cell growth. This could be due to a nutrient deficiency from BBM, as the $CaCl_2$ crosslinking process could have diminished the BBM content in the hydrogel without any subsequent BBM addition. The hydrogel of Category IV showed an increasing green trend from day 2 to day 5, but it turned yellowish afterwards. This could be because the BBM initially present in the hydrogel was able to support *C. vulgaris* cell growth until day 5, after which it was depleted, leading to a nutrient shortage among the cells.

The ΔRGB values for each sample were determined, and the cell concentrations of the samples were calculated using the ΔRGB values tabulated in Fig. 1(d). The growth curve of *C. vulgaris* in each category of hydrogel over a 10-day cultivation period was plotted, as shown in Fig. 3(a). Categories I and II are also plotted despite having inconsistent data due to drying of the hydrogel during the cultivation period. The growth curve revealed a gradual increase in ΔRGB intensity in Category III compared to other categories. The lag phase lasted for 3 days, after which the cell concentration began to increase from day 4 to day 8, marking the exponential phase. On day 8, the growth of *C. vulgaris* transitioned into the stationary phase. For Category I, despite the hydrogel dehydration that occurred, cell cultivation still proceeded well within three days. Based on Fig. 2, cell growth was faster compared to Category III, and the growth curve entered the exponential phase starting from the first day of cultivation. In contrast, the other categories, namely II, IV and V, showed lower ΔRGB values, corresponding to less noticeable color changes.

The growth curve of *C. vulgaris* cultivated conventionally was compared with that of Category III cultivated in the hydrogel system, as depicted in Fig. 3(b). Category III was selected for this comparison due to its superior growth curves relative to other categories. The exponential phase of *C. vulgaris* in hydrogel was compared between the conventional and hydrogel growth curve, taking into account the growth trend of *C. vulgaris*. Given the more stable growth curve of *C. vulgaris* in the Category III hydrogel, its exponential phase lasted until the 8^{th} day. This suggests that the peak growth rate of *C. vulgaris* cultivated in this hydrogel can be reached within 8 days. This duration is notably shorter compared to the 11-day exponential phase seen in the growth curve of *C. vulgaris* cultivated using conventional methods, as shown in Fig. 3(b). A prolonged exponential phase can be

beneficial as it allows cells more time for nutrient absorption and cell division, leading to a higher biomass yield (Iwamoto *et al.* 2014).

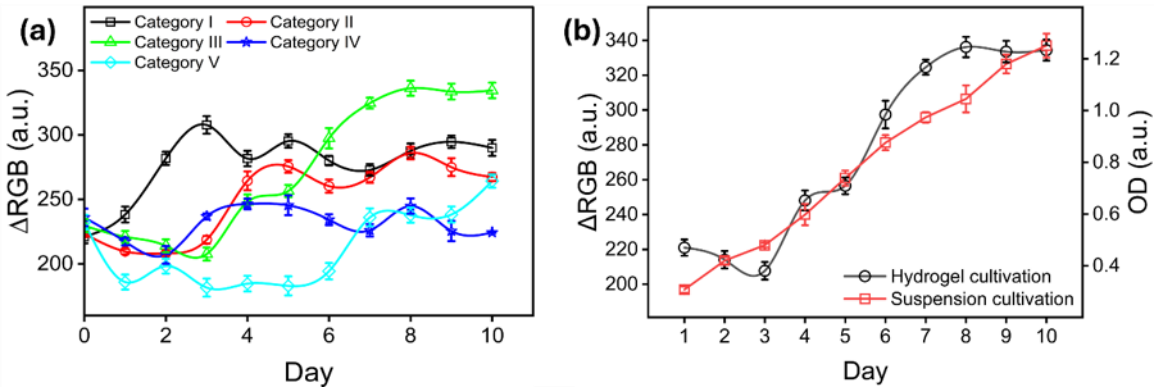

Fig. 3. (a) Growth curve of *C. vulgaris* cultivated in hydrogel of different categories based on ΔRGB values from colorimetric analysis and (b) comparison of growth curve of *C. vulgaris* cultivated through conventional and Category III hydrogel cultivation methods

Conversely, a shorter exponential phase enhances resource efficiency by demanding less nutrients, energy, and shorter cultivation duration. Additionally, a shorter exponential phase indicates that the cell is healthy and can aid in inhibiting the proliferation of contaminants, thus minimizing contamination risk (Zhang *et al.* 2020). As such, the cultivation of cells in the hydrogel continues to be a subject of ongoing research and investigation. Its distinctive properties and potential benefits over conventional methods make it a compelling area of study. For further studies related to 3D bioprinting, hydrogels from Categories I and III provide a more conducive environment for the growth of *C. vulgaris* cells. Therefore, the hydrogel preparation technique and cultivation conditions used in Category I were applied in the subsequent 3D bioprinting process with the control environment.

Structure Stability of 3D Bioprinted CNF/CMC with *C. vulgaris*

The structure created by 3D printing of each distinct CNF and CMC concentration ratio is analyzed from both top and side views based on the physical structure and the dimension, as depicted in Fig. 4 and Table 3. Observations conducted immediately after the printing process reveal that the printing of CNF, CMC, and CNF/CMC can be performed successfully without complications, maintaining the rigidity of both the biomaterial ink and the final 3D printed material. The printed constructs exhibited excellent structural fidelity without any signs of collapse. This successful shape retention aligns with the rheological behavior established in our previous report (Sajab *et al.* 2024), which demonstrated that these composites exhibit a higher storage modulus (G') compared to their loss modulus (G''). This dominant solid-like characteristic ensures that the printing solution can rapidly recover and maintain its shape post-extrusion during the DIW 3D printing process.

The observation was conducted immediately after the printing process. The results reveal that the printing process of CNF, CMC, and CNF/CMC can be performed successfully without complications, maintaining the rigidity of the biomaterial ink, as well as 3D-printed material.

The 3D printed constructs composed of hydrogel with a higher concentration ratio of CMC (CNF/CMC 4:5, CNF/CMC 4:6, and CNF/CMC 5:6) exhibited a less rigid structure. Among the three ratios, the hydrogel structure with CNF/CMC 4:6 was the most unstable and prone to collapse due to the high solubility and hygroscopicity of CMC (Chen *et al.* 2020). Consequently, the increased volume of CMC dispersed in the BBM solution, also leading to the formation of a less viscous and unstable hydrogel. Although the hydrogel with CNF/CMC 5:6 appeared rigid from the side view, its structure gradually collapses over time. Meanwhile the increase in CNF concentration (CNF/CMC 4:5, CNF/CMC 5:5, and CNF/CMC 6:5) showed a better 3D-printed structure.

The dimensional details of the 3D-printed structure are tabulated in Table 3, presenting the differences in width, length, outer grid width, inner grid width, and thickness for different concentration ratios of CNF and CMC. Inner grid width is the crucial dimension parameter in explaining the printability and shape fidelity. The study concludes that the larger the size of inner grid leads to the collapse of printed structure, which can be clearly seen through CNF/CMC 4:6 in Fig. 5, with 6.598±0.052 cm.

Meanwhile, CNF/CMC 5:5 and CNF/CMC 6:5 showed the best inner grid width and good printing with the lowest value of 3.763±0.026 cm and 3.829±0.075 cm, respectively. For the hydrogel CNF/CMC 6:5, the structure of the 3D-printed hydrogel was rigid and showed the highest thickness of 3.920±0.025 cm, followed by CNF/CMC 5:6. However, the shape slightly deviated from the original design and progressively underwent structural failure, which could be due to the higher concentration ratio of CNF in the hydrogel. It was observed that over time, CNF/CMC 5:5 exhibited the best shape fidelity without causing any structural degradation, although the thickness within the medium ranges.

An increased composition of CNF could result in a larger intrinsic viscosity of the hydrogel, causing poor fluidity of the hydrogel through the nozzle, thereby impacting the bioprinting process and the final shape (Orelma *et al.* 2017; Leppänen *et al.* 2020). Too high concentration would cause a defect in the printed structure. Among the five different concentration ratios, the construct of CNF/CMC 5:5 hydrogel exhibited the most rigid and best printed structure. The gap between the designed wall and the ability to maintain the structure without collapsing can be clearly seen from Fig. 4. Thus, it can be concluded that a hydrogel with this concentration ratio is suitable for obtaining a rigid and stable 3D-bioprinted hydrogel.

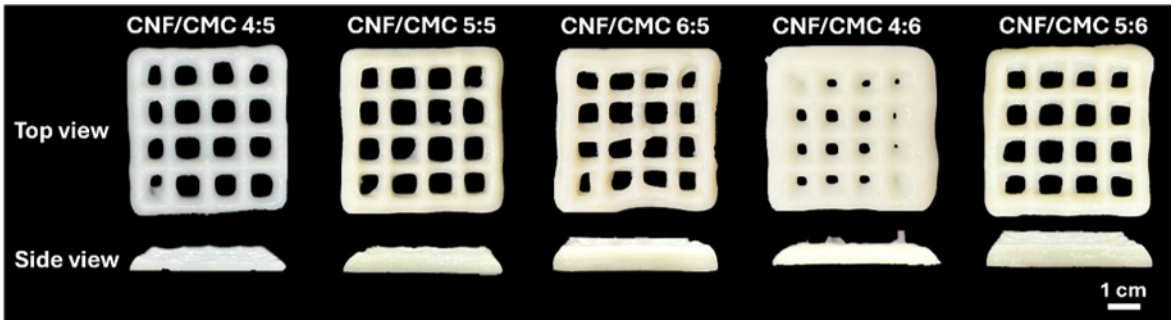

Fig. 4. Structure stability and rigidity of 3D-bioprinted *C. vulgaris* in CNF/CMC hydrogel system at different composition ratios

Table 3. Dimension of 3D Printed Hydrogel Based on Different Concentration Ratio of CNF/CMC

Dimension	CNF/CMC 4:5	CNF/CMC 5:5	CNF/CMC 6:5	CNF/CMC 4:6	CNF/CMC 5:6
Width	4.802	4.901	4.838	5.189	5.036
Length	5.047	5.009	5.000	4.920	5.153
Outer grid width	5.456±0.053	5.672±0.045	6.673±0.049	9.863±0.141	6.428±0.079
Inner grid width	4.226±0.043	3.763±0.026	3.829±0.075	6.598±0.052	4.277±0.033
Thickness	1.743±0.062	2.993±0.038	3.920±0.025	2.714±0.027	3.356±0.043

3D Bioprinting on the Microalgae Cultivation

A rheology test on the 3D printing ink was conducted to understand its rheological properties of the biomaterial using the CNF (6 wt%), CMC (5 wt%), and CNF/CMC (6 : 5 wt%). The shear rate of CNF, CMC, and CNF/CMC at 0.1 s^{-1} was at the minimum value 35, 140, and 111 Pa and increased as the shear rate increased (Fig. 5(a)). However, the shear stress of CNF was maintained at its initial state and only elevated slightly to 141 Pa. It is noticeable that CMC achieved the highest shear rate due to the high thickness of the ink. This is supported by the viscosity of the biomaterial ink in Fig. 5(b), where the CMC showed the highest reading. The viscosity of the ink was at the maximum at low shear rate and it noticeably decreased as the shear rate increased. Based on the plotted flow curves and viscosity in Fig. 5(a) and (b), the biomaterial ink exhibited a non-Newtonian fluid characteristic and shear thinning behaviour (Jyoti *et al.* 2013; Lee *et al.* 2017). This rheological study was limited to observing the shear thinning behaviour of the hydrogel, and future work is recommended to include a yield stress test and the recovery behaviour to further enhance the understanding of the ink properties.

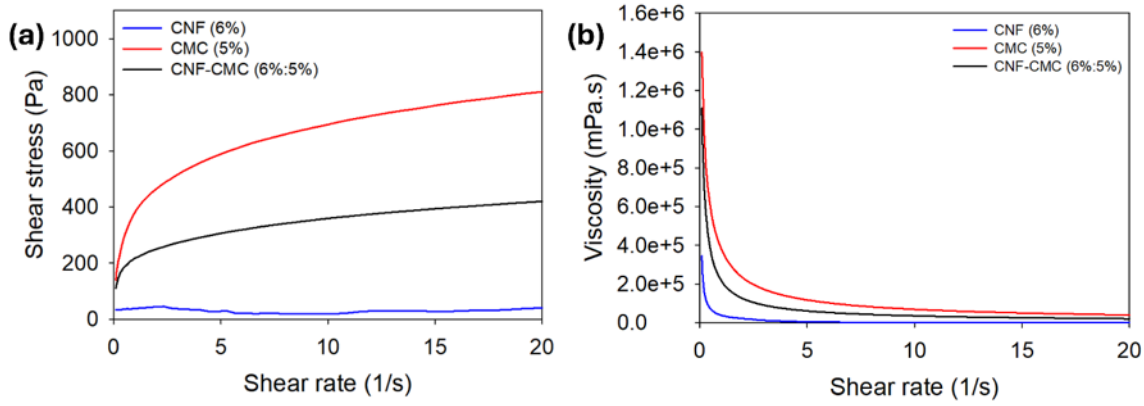

Fig. 5. The rheological properties of the biomaterial ink: (a) Flow curves shear stress (Pa) as the function of shear rate (1/s); (b) The viscosity (mPa.s) as the function of shear rate (1/s)

In addition to examining the impact of CNF and CMC ratios on 3D bioprinting, the growth of *C. vulgaris* was also studied using the same 3D-printed hydrogel. The growth patterns of *C. vulgaris* in hydrogels with varying concentration ratios under Category I condition over a period of 7 days are depicted in Fig. 6(a). An earlier experiment with a CNF/CMC 4:5 hydrogel revealed that the hydrogel dried out quickly within a day. Further exploration indicated that this was due to the heat from the nearby light source, which accelerated the evaporation from the uncovered petri dish containing the bioprinted

hydrogel. As a result, in subsequent experiments with different CNF and CMC compositions, the petri dish was covered to reduce evaporation and slow the hydrogel's drying rate, ensuring more reliable and consistent results.

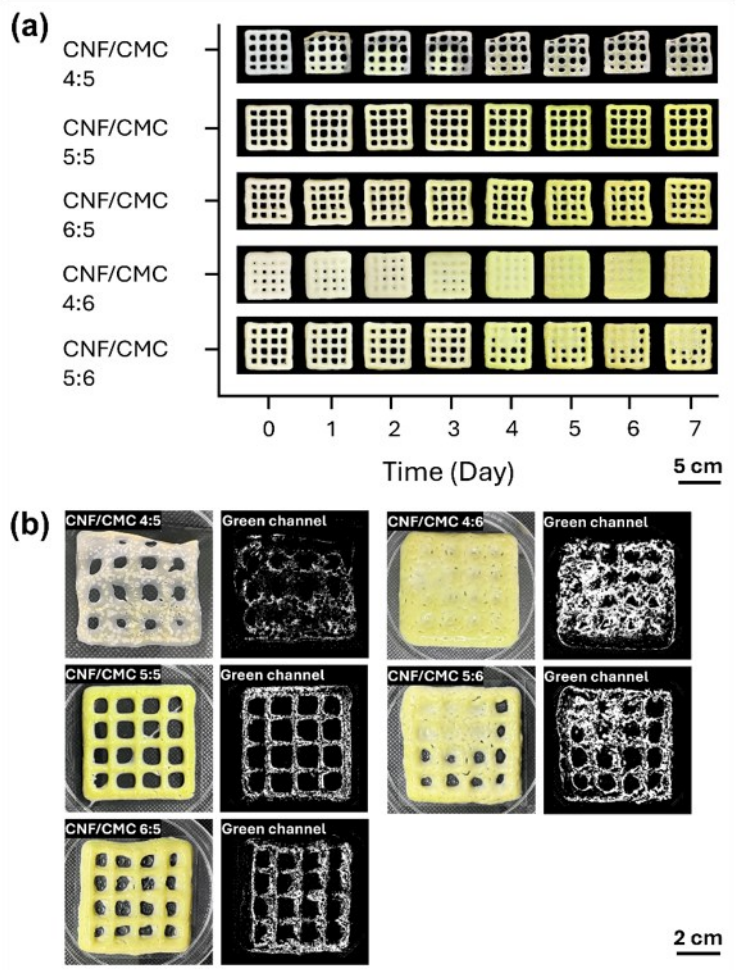

Fig. 6. Observation of *C. vulgaris* cell growth (Category I): (a) The growth of 3D-bioprinted CNF/CMC hydrogel; (b) ImageJ software analysis on CNF/CMC hydrogel at different ratio

In Category I, there was a gradual intensification of the green color over time in the 3D-bioprinted hydrogel, except for the one composed of 4 wt% CNF and 5 wt% CMC. This particular hydrogel showed only a minor shift to green, indicating minimal *C. vulgaris* growth, possibly due to the evaporation of BBM after the hydrogel dried. However, for CNF/CMC 6:5, CNF/CMC 4:6, and CNF/CMC 5:6 hydrogels, the green color increased until day 5 before turning slightly yellowish green, suggesting unfavorable *C. vulgaris* growth from 5th day and onwards. Of all the concentration ratios, only the 3D-printed hydrogel with CNF/CMC 5:5 demonstrated a continuous green color increase until day 7, in addition to maintaining a good 3D-printed shape.

The change in color of hydrogel cultures from green to yellowish green after 3D bioprinting is likely due to several factors. The first factor may be contamination, as hydrogels for 3D bioprinting require multiple and tedious processes. The exposure of the culture media to contaminants is higher during the preparation and printing process. The second factor is excessive light exposure, which causes the acclimation process. Excessive light exposure causes *C. vulgaris* to start producing pigments such as xanthophyll and

zeaxanthin (Grudzinski *et al.* 2016). Xanthophyll is an active ingredient that acts as an antioxidant, while zeaxanthin is a pigment that can protect the eyes from macular degeneration.

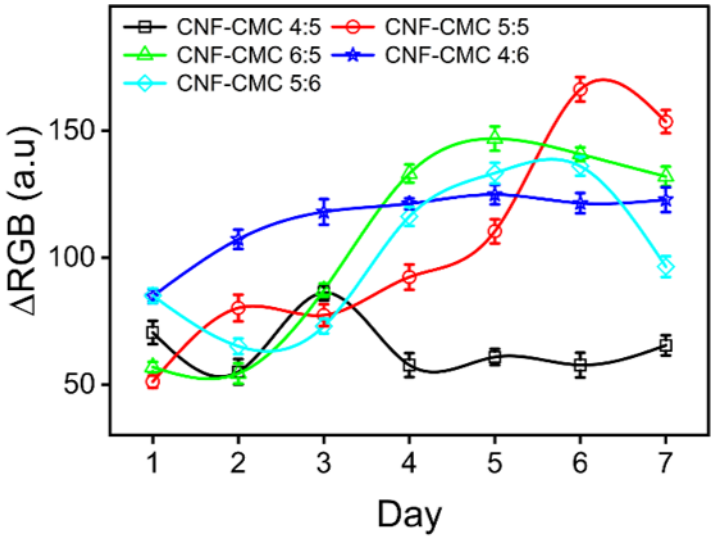

Fig. 7. Growth curves of *C. vulgaris* cells in 3D-bioprinted hydrogels with varying CNF/CMC concentration ratios under Category I cultivation conditions

Table 4. Comparison of Cell Growth for Various Biopolymer Composition in Cultivating Microalgae Cells

Polymer	Living Cells	Printability	Cell Growth	Reference
Alginate/ methylcellulose scaffold	*Chlamydomonas reinhardtii*	Yes	Rapid increase in oxygen production: 0.05 to 0.25 mg/Lh in 2 days.	(Lode *et al.* 2015)
Calcium-alginate hydrogel	*Synechococcus elongatus* PCC 7942	No	Optimum harvest period in 2 to 3 days. Peak productivity: 1.0 gDW/m^{2}d	(Pierobon *et al.* 2017)
Alginate beads	*Scenedesmus obliquus* and *Chlorella vulgaris*	No	Cells have high growth near the bead's surfaces.	(Ruiz-Marin *et al.* 2010)
Alginate beads	*Chlorella vulgaris* and *Chlorella* sp.	No	Significant increase in intracellular density within 10 days. Granule turns deep green with no physical changes.	(Wu *et al.* 2020)
Gelatin hydrogel	*Marinichlorella kaistiae* KAS603 and bacteria, *Erythrobacter sp*	No	Obtained 2.85×10^7 cells/mL in 3 days. Obvious green color changes for co-culture.	(Martin *et al.* 2021)
Alginate/silica hydrogel	*Chlorella vulgaris*	Yes	Cells can remain viable and proliferate for several weeks.	(Pannier *et al.* 2014)

Furthermore, the distribution and density of microalgae cells across different hydrogel formulations were compared using ImageJ analysis, specifically by evaluating the white-colored areas generated from the green color channel (Fig. 6(b)). The CNF/CMC 4:5 formulation exhibited considerably fewer white spots compared to the other

combinations, indicating a lower concentration of detectable green cells. This lower cell density corresponds directly to the lighter green hue observed in the original physical images of the CNF/CMC 4:5 sample. The other formulations have more white spots referring to the microalgae cells, especially CNF/CMC 5:5 where the generated result completely following the original image. This situation explained the uniform growth of microalgae cells on the entire 3D-bioprinted material surfaces. This is also supported by the increases of ΔRGB value on day 5 and 6 as shown in Fig. 7. The CNF/CMC 5:5 concentration ratio has the highest ΔRGB value among the others concentration. Moreover, a comparison of microalgae and human cell growth in different biopolymer composition is tabulated in Table 4.

Micrograph of 3D-bioprinted Hydrogel

The morphological analysis of *C. vulgaris* culture, CNF/CMC hydrogel, and CNF/CMC hydrogel with *C. vulgaris* cells was conducted using optical microscope and FESEM to gain a deeper understanding of the hydrogel and *C. vulgaris* structures. In Fig. 8(a) and (b), the *C. vulgaris* cells are seen to have an elongated cylindrical shape with small particles visibly attached to their surface. *C. vulgaris* typically has irregular shapes with cavities attached to the cell surfaces and folded cell walls (Elumalai *et al.* 2011; Maliutina *et al.* 2018). The image of raw *C. vulgaris* obtained aligns with the cell shape and structure found in previous studies. As shown in Fig. 8(c), the CNF/CMC hydrogel exhibited a structure with large pores and walls. This is attributed to the freeze-drying process used during sample preparation, which can create up to 99% pores as it removes unbound water from the hydrogel (Mirtaghavi *et al.* 2020). The increased porosity post freeze-drying provides ample space for the growth of *C. vulgaris* cells within the hydrogel.

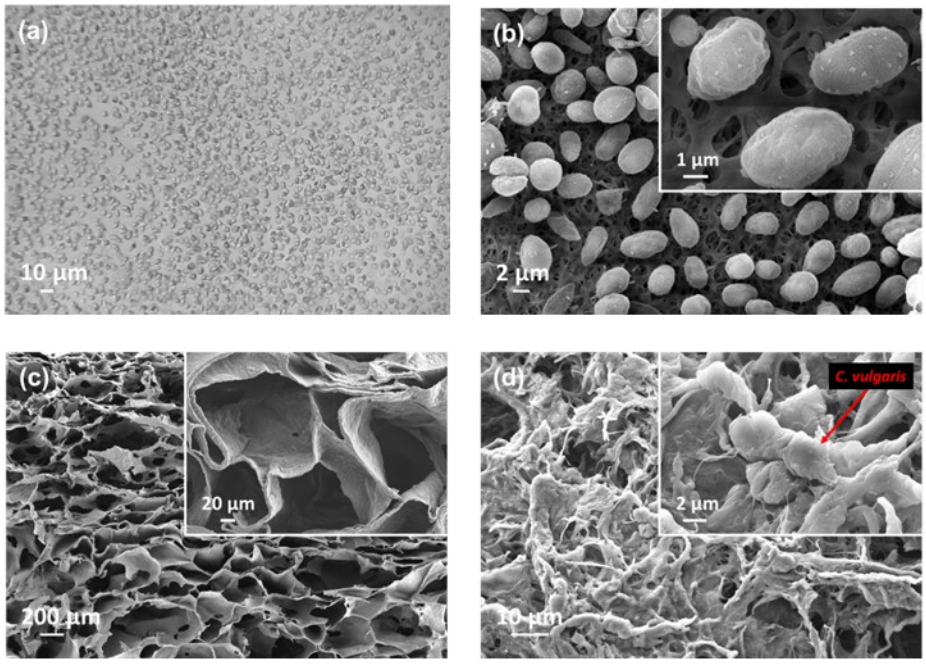

Fig. 8. Optical microscope image of (a) *C. vulgaris* culture and FESEM micrograph images of (b) *C. vulgaris* culture, (c) CNF/CMC hydrogel, and (d) CNF/CMC hydrogel containing *C. vulgaris* cells

Figure 8(d) shows *C. vulgaris* cells attached to the hydrogel structure during growth, illustrating immobilized *C. vulgaris* during the cultivation process. The cell structure is not clearly visible, as it is covered by the CNF/CMC hydrogel. A similar morphological view of cell attachment in collagen hydrogel from another study confirms the presence of *C. vulgaris* cells in Fig. 8(c) (Mahmoodi *et al.* 2021). Despite the morphology indicating complete entrapment of *C. vulgaris* cells in the hydrogel, the cells were able to grow, demonstrating the suitability and compatibility of the biomaterial used.

CONCLUSIONS

Natural resources derived from oil palm empty fruit bunch (OPEFB) hold great potential as bioink for 3D bioprinting, particularly with the incorporation of living cells. The study findings suggest a high compatibility of microalgae printed in cellulose-based hydrogel.

1. The cellulose nanofiber/carboxymethyl cellulose (CNF/CMC) 5:5 hydrogel exhibited superior structural rigidity in 3D bioprinting application and is most conducive to the growth of *C. vulgaris* based on the green hue observed after 5 days of cultivation.
2. Colorimetric analysis is an effective method for understanding microalgae growth within the hydrogel cultivation system by the detection of color changes through the red-green-blue (RGB) values.
3. Microalgae cultivation in hydrogel system exhibited a faster growth rate by achieving the exponential phase within 8 days compared to the suspension system in 11 days, supported by the immobilized of cell within the hydrogel matrix surrounded with nutrient for easy food access.

ACKNOWLEDGMENTS

The authors are grateful for the support of the Ministry of Higher Education (MoHE) Malaysia and Universiti Kebangsaan Malaysia, Exploratory and Transformative Research Grant (GET/2026/04854) and (GUP-2024-063). During the preparation of this work, the authors used Google Gemini (Version 3.1 Pro) to improve language and readability. After using this tool, the authors have reviewed and edited the content as needed and take full responsibility for the content of the publication.

Conflict of Interest

Authors declare no conflicts of interest that could potentially be affected by the publication of their manuscript.

REFERENCES CITED

Anderson, R. A. (2005). *Algal Culturing Techniques*, First Ed., Academic Press, Amsterdam, Netherlands.

Badhe, R. V., and Nipate, S. S. (2020). "Cellulosic materials as bioinks for 3D printing applications," in: *Advanced 3D-Printed Systems and Nanosystems for Drug Delivery and Tissue Engineering*, Elsevier Inc., Amsterdam, Netherlands, pp. 109-137.

Chen, F., Sawada, D., Hummel, M., Sixta, H., and Budtova, T. (2020). "Unidirectional all-cellulose composites from flax *via* controlled impregnation with ionic liquid," *Polymers* 12(5), article 1010. https://doi.org/10.3390/polym12051010

Cohen, Y. (2001). "Biofiltration – The treatment of fluids by microorganisms immobilized into the filter bedding material: A review," *Bioresource Technology* 77, 257-274. https://doi.org/10.1016/S0960-8524(00)00074-2

Dishon, G., Resetarits, H. M., Tsai, B., Black, K., Grossmann, J., and Smith, J. E. (2022). "Image-based analysis and quantification of biofouling in cultures of the red alga *Asparagopsis taxiformis*," *Journal of Applied Phycology* 35, 209-218. https://doi.org/10.1007/s10811-022-02884-y

Elumalai, S., Baskaran, S., Prakasam, V., and Kumar, N. S. (2011). "Ultra-structural analysis and lipid staining of biodiesel-producing microalgae *Chlorella vulgaris* collected from various ponds in Tamil Nadu, India," *Journal of Ecobiotechnology* 2, 5-7. https://doi.org/10.5958/j.0976-3015.2.2.004

Ergun, R., Guo, J., and Huebner-Keese, B. (2016). "Cellulose," in: *Encyclopedia of Food and Health*, Academic Press, Oxford, UK, pp. 694-702. https://doi.org/10.1016/B978-0-12-384947-2.00127-6

Gopinathan, J., and Noh, I. (2018). "Recent trends in bioinks for 3D printing," *Biomaterials Research* 22, 1-15. https://doi.org/10.1186/s40824-018-0122-1

Grudzinski, W., Krzeminska, I., Luchowski, R., Nosalewicz, A., and Gruszecki, W. I. (2016). "Strong-light-induced yellowing of green microalgae Chlorella: A study on molecular mechanisms of the acclimation response," *Algal Research* 16, 245-254.

Hlaing, W. M. M., Kruanetr, S., and Ruengsitagoon, W. (2020). "RGB colorimetric method for the quantitative analysis of levocetirizine tablets," *Isan Journal of Pharmaceutical Sciences (IJPS)* 16, 78-88. https://doi.org/10.14456/ijps.2020.19

Iwamoto, S., Lee, S. H., and Endo, T. (2014). "Relationship between aspect ratio and suspension viscosity of wood cellulose nanofibers," *Polymer Journal* 46, 73-76. https://doi.org/10.1038/pj.2013.64

Jorfi, M., and Foster, E. J. (2015). "Recent advances in nanocellulose for biomedical applications," *Journal of Applied Polymer Science* 132, article 4179. https://doi.org/10.1002/app.41719

Jyoti, B. V. S., Varma, M., and Baek, S. W. (2013). "Comparative study of rheological properties of ethanol and UDMH based gel propellants," in: *5th European Conference for Aeronautics and Space Sciences (EUCASS)*, Munich, Germany.

Kargarzadeh, H., Mariano, M., Huang, J., Lin, N., Ahmad, I., Dufresne, A., and Thomas, S. (2017). "Recent developments on nanocellulose reinforced polymer nanocomposites: A review," *Polymer* 132, 368-393. https://doi.org/10.1016/j.polymer.2017.09.043

Krujatz, F., Lode, A., Brüggemeier, S., Schütz, K., Kramer, J., Bley, T., Gelinsky, M., and Weber, J. (2015). "Green bioprinting: Viability and growth analysis of microalgae immobilized in 3D-plotted hydrogels *versus* suspension cultures," *Engineering in Life Sciences* 15, 678-688. https://doi.org/10.1002/elsc.201400131

Landers, R., Hübner, U., Schmelzeisen, R., and Mülhaupt, R. (2002). "Rapid prototyping of scaffolds derived from thermoreversible hydrogels and tailored for applications in

tissue engineering," *Biomaterials* 23, 4437-4447. https://doi.org/10.1016/S0142-9612(02)00139-4

Lee, J. K., Ko, J., and Kim, Y. S. (2017). "Rheology of fly ash mixed tailings slurries and applicability of prediction models," *Minerals* 7(9), 1-10.

Leppänen, I., Hokkanen, A. Österberg, M., Vähä-Nissi, M., Harlin, A., and Orelma, H. (2022). "Hybrid films from cellulose nanomaterials—Properties and defined optical patterns," *Cellulose* 29, 8551-8567. https://doi.org/10.1007/s10570-022-04795-0

Lode, A., Krujatz, F., Brüggemeier, S., Quade, M., Schütz, K., Knaack, S., Weber, J., Bley, T., and Gelinsky, M. (2015). "Green bioprinting: Fabrication of photosynthetic algae-laden hydrogel scaffolds for biotechnological and medical applications," *Engineering in Life Sciences* 15, 177-183.

Mahmoodi, N., Ai, J., Hassannejad, Z., Ebrahimi-Barough, S., Hasanzadeh, E., Nekounam, H., Vaccaro, A. R., and Rahimi-Movaghar, V. (2021). "Improving motor neuron-like cell differentiation of hEnSCs by the combination of epothilone B-loaded PCL microspheres in optimized 3D collagen hydrogel," *Scientific Reports* 11, 1-22. https://doi.org/10.1038/s41598-021-01071-2

Maliutina, K., Tahmasebi, A., and Yu, J. (2018). "Effects of pressure on morphology and structure of bio-char from pressurized entrained-flow pyrolysis of microalgae," *Data in Brief* 18, 422-431. https://doi.org/10.1016/j.dib.2018.03.048

Martin, N., Bernat, T., Dinasquet, J., Stofko, A., Damon, A., Deheyn, D. D., Farooq, A., Smith, J. E., Davey, M. P., Smith, A. G., *et al.* (2021). "Synthetic algal-bacteria consortia for space-efficient microalgal growth in a simple hydrogel system," *Journal of Applied Phycology* 33, 2805-2815. https://doi.org/10.1007/s10811-021-02528-7

Mirtaghavi, A., Luo, J., and Muthuraj, R. (2020). "Recent advances in porous 3D cellulose aerogels for tissue engineering applications: A review," *Journal of Composites Science* 4, article 152. https://doi.org/10.3390/jcs4040152

Mohan, D., Khairullah, N. F., How, Y. P., Sajab, M. S., and Kaco, H. (2020). "3D printed laminated $CaCO_3$–nanocellulose films as controlled-release 5-fluorouracil," *Polymers* 12(4), article 986. https://doi.org/10.3390/polym12040986

Mohan, D., Teong, Z. K., Sajab, M. S., Kamarudin, N. H. N., and Kaco, H. (2021). "Intact fibrillated 3D-printed cellulose macrofibrils/$CaCO_3$ for controlled drug delivery," *Polymers* 13(12), article 1912. https://doi.org/10.3390/polym13121912

Nan, N. F. C., Zainuddin, N., and Ahmad, M. (2019). "Preparation and swelling study of CMC hydrogel as potential superabsorbent," *Pertanika Journal of Science and Technology* 27, 489-498.

Nasution, H., Harahap, H., Dalimunthe, N. F., Ginting, M. H. S., Jaafar, M., Tan, O. O. H., Aruan, H. K., and Herfananda, A. L. (2022). "Hydrogel and effects of crosslinking agent on cellulose-based hydrogels: A review," *Gels* 8(9), article 568. https://doi.org/10.3390/gels8090568

Orelma, H., Korpela, A., Kunnari, V., Harlin, A., and Suurnäkki, A. (2017). "Improving the mechanical properties of CNF films by NMMO partial dissolution with hot calender activation," *Cellulose* 24, 1691-1704. https://doi.org/10.1007/s10570-017-1229-6

Pannier, A., Soltmann, U., Soltmann, B., Altenburger, R., and Schmitt-Jansen, M. (2014). "Alginate/silica hybrid materials for immobilization of green microalgae *Chlorella vulgaris* for cell-based sensor arrays," *Journal of Materials Chemistry B* 2, 7896-7909. https://doi.org/10.1039/c4tb00944d

Pazzi, B. M., Pistoia, D., and Alberti, G. (2022). "RGB-Detector: A smart, low-cost device for reading RGB indexes of microfluidic paper-based analytical devices," *Micromachines* 13(10), article 1585. https://doi.org/10.3390/mi13101585

Pierobon, S. C., Riordon, J., Nguyen, B., Ooms, M. D., and Sinton, D. (2017). "Periodic harvesting of microalgae from calcium alginate hydrogels for sustained high-density production," *Biotechnology and Bioengineering* 114, 2023-2031. https://doi.org/10.1002/bit.26325

Ramadan, Q., and Zourob, M. (2021). "3D Bioprinting at the frontier of regenerative medicine, pharmaceutical, and food industries," *Frontiers in Medical Technology* 2, article 607648. https://doi.org/10.3389/fmedt.2020.607648

Ruiz-Marin, A., Mendoza-Espinosa, L. G., and Stephenson, T. (2010). "Growth and nutrient removal in free and immobilized green algae in batch and semi-continuous cultures treating real wastewater," *Bioresource Technology* 101, 58-64. https://doi.org/10.1016/j.biortech.2009.02.076

Sajab, M. S., Mohan, D., Santanaraj, J., Chia, C. H., Kaco, H., Harun, S., and Kamarudin, N. H. N. (2019). "Telescopic synthesis of cellulose nanofibrils with a stable dispersion of Fe(0) nanoparticles for synergistic removal of 5-fluorouracil," *Scientific Reports* 9, article 11703. https://doi.org/10.1038/s41598-019-48274-2

Sajab, M. S., Mohan, D., Ling, T. T., Kaco, H., Ishak, W. H. W., and Ding, G. (2024). "Nanocellulose-based composites for 3D printed stimuli-responsive swelling hydrogel," *Industrial Crops and Products* 222, article 119541. https://doi.org/10.1016/j.indcrop.2024.119541

Shaghaleh, H., Xu, X., and Wang, S. (2018). "Current progress in production of biopolymeric materials based on cellulose, cellulose nanofibers, and cellulose derivatives," *RSC Advances* 8, 825-842. https://doi.org/10.1039/c7ra11157f

Show, P. L., Tan, J. S., Lee, S. Y., Chew, K. W., Lam, M. K., Lim, J. W., and Ho, S. (2020). "A review on microalgae cultivation and harvesting, and their biomass extraction processing using ionic liquids," *Bioengineered* 11, 116-129. https://doi.org/10.1080/21655979.2020.1711626

Sood, S., Singhal, R., Bhat, S., and Kumar, A. (2011). "Inoculum preparation," in: *Comprehensive Biotechnology*, 2nd Ed., Elsevier B.V., Amsterdam, Netherlands, pp. 152-164.

Stanbury, P. F., Whitaker, A., and Hall, S. J. (2017). "Chapter 2 – Microbial growth kinetics," in: *Principles of Fermentation Technology*, 3rd Ed., Elsevier, Amsterdam, Netherlands, pp. 21-74.

Vurat, M. T., Şeker, Ş., Lalegül-Ülker, Ö., Parmaksiz, M., Elçin, A. E., and Elçin, Y. M. (2022). "Development of a multicellular 3D-bioprinted microtissue model of human periodontal ligament-alveolar bone biointerface: Towards a pre-clinical model of periodontal diseases and personalized periodontal tissue engineering," *Genes and Diseases* 9, 1008-1023. https://doi.org/10.1016/j.gendis.2020.11.011

Wan Jusoh, W. N. L., Sajab, M. S., Mohd Yasin, N. H., Abdul, P. M., and Takriff, M. S. (2025). "Interaction of *Chlorella vulgaris*: Cell attachment on nanocellulose-based hydrogel for sustainable microalgae cultivation," *BioResources* 20(1), 201-218. https://doi.org/10.15376/biores.20.1.201-218

Wirth, R., Pap, B., Böjti, T., Shetty, P., Lakatos, G., Bagi, Z., Kovács, K. L., and Maróti, G. (2020). "*Chlorella vulgaris* and its phycosphere in wastewater: Microalgae–bacteria interactions during nutrient removal," *Frontiers in Bioengineering and Biotechnology* 8, article 557572. https://doi.org/10.3389/fbioe.2020.557572

Wu, J. Y., Lay, C. H., Chiong, M. C., Chew, K. W., Chen, C. C., Wu, S. Y., Zhou, D., Kumar, G., and Show, P. L. (2020). "Immobilized *Chlorella* species mixotrophic cultivation at various textile wastewater concentrations," *Journal of Water Process Engineering* 38, article 101609. https://doi.org/10.1016/j.jwpe.2020.101609

Yatirajula, S. K., Shrivastava, A., Saxena, V. K., Kodavaty, J. (2019). "Flow behavior analysis of *Chlorella vulgaris* microalgal biomass," *Heliyon* 5, article e01845. https://doi.org/10.1016/j.heliyon.2019.e01845

Zainal, S. H., Nofrianti, R., Lazim, A. M., and Othaman, R. (2019). "Cellulose-based hydrogel as halal agricultural medium," *Malaysian Applied Biology* 48(2), 109-113.

Zhang, S., Li, G., Man, J., Zhang, S., Li, J., Li, J., and Li, D. (2020). "Fabrication of microspheres from high-viscosity bioink using a novel microfluidic-based 3D bioprinting nozzle," *Micromachines* 11(7), article 681. https://doi.org/10.3390/mi11070681

Article submitted: February 28, 2026; Peer review completed: April 18, 2026; Revised version received: April 27, 2026; Accepted: August 3, 2026; Published: August 14, 2026.
DOI: 10.15376/biores.21.4.9761-9779